Uzawa Block Relaxation Domain Decomposition Method for the Two-Body Contact Problem With Tresca Friction

Jonas Koko

Uzawa Block Relaxation Domain Decomposition Method for the Two-Body Contact Problem With Tresca Friction

Jonas Koko[1]

Research Report LIMOS/RR-08-01

15 janvier 2008

[1]LIMOS, Université Blaise Pascal – CNRS UMR 6158, Campus des Cézeaux B.P. 10125, 63173 Aubière cedex, France; e-mail: koko@isima.fr

Abstract

We propose a Uzawa block relaxation domain decomposition method for a two-body contact problem with Tresca friction. We introduce auxiliary interface unknowns to transform the variational problem into a saddle-point problem. Applying a Uzawa block relaxation algorithm to the corresponding augmented Lagrangian functional we obtain a domain decomposition algorithm in which we have to solve two uncoupled linear elasticity subproblems in each iteration. The auxiliary unknowns are computed explicitly using Kuhn-Tucker conditions and Fenchel duality theory. Numerical experiments show the scalability of the domain decomposition algorithm on matching or nonmatching meshes for two- or three-dimensional contact problems.

Keywords: Two-body contact, augmented Lagrangian, Kuhn-Tucker conditions, Fenchel duality, domain decomposition

1 Introduction

Various domain decomposition methods, for contact problems, have been proposed by many authors in order to speed up the solution. Dostal et al. [7] have proposed an augmented Lagrangian/domain decomposition method. The scalability of the method has been studied by Schöberl [28], Dureisseix and Farhat [9], Dostál and Horák [6]. The methods presented in [9, 7, 6, 28] are based on the FETI domain decomposition method [11] and designed on the discrete level. Kosior et al. [23] have proposed a domain decomposition method based on boundary element techniques. Bayada et al. have proposed Neumann-Neumann [2] and a Neumann-Dirichlet [1] domain decomposition algorithms. Koko [20] has proposed a domain decomposition method based on the decomposition of the set of admissible displacements introduced by the nonpenetration condition. Note that the domain decomposition proposed in [1, 2, 20] are designed on the continuous problem.

We propose in this paper an augmented Lagrangian based domain decomposition method for the two-body contact problem with Tresca friction, designed on the continuous level. Auxiliary unknowns are introduced to separate the subdomains representing the linear elastic bodies, leading to a constrained (convex) minimization formulation. Applying a Uzawa block relaxation method to the corresponding augmented Lagrangian functional yields a domain decomposition method in which we have to solve two uncoupled linear elasticity subproblems in every iteration. The auxiliary unknowns are computed explicitly using Kuhn-Tucker and Fenchel duality. The domain decomposition presented in this article is an operator-splitting type method [12, 13]. We refer to [5] for block relaxation method in convex minimization and to [26] (and references therein) for Lagrange multiplier based domain decomposition methods. The Tresca friction problem is a commonly chosen approach towards the solution of the Coulomb frictional contact problem through fixed-point procedures (see e.g. [8, 15, 24]).

The paper is organized as follows. In Section 2 we state the two-body contact problem with Tresca friction. The Uzawa block relaxation domain decomposition algorithm is described in Section 3 followed by the convergence results in Section 4. In Section 5 we report numerical experiments carried out with the new algorithm.

2 Problem statement

We consider two elastic bodies each of them occupying a bounded domain Ω^α in $\mathbb{R}^d$, $d \geq 2$ and $\alpha = 1, 2$. We denote by Γ^α the boundary of Ω^α, assumed to be "sufficiently" smooth. We assume that $\Gamma^\alpha = \Gamma_D^\alpha \cup \Gamma_N^\alpha \cup \Gamma_c^\alpha$ where $\{\Gamma_D^\alpha, \Gamma_N^\alpha, \Gamma_c^\alpha\}$ is a partition of Γ^α with $\mathrm{mes}(\Gamma_D^\alpha) > 0$ and $\mathrm{mes}(\Gamma_c^\alpha) > 0$. On Γ_D^α a displacement is prescribed while on Γ_N^α a surface traction is prescribed. Γ_c^α is a part of Γ^α where both bodies may come in contact in the deformed configuration.

2.1 Equilibrium equations

Let $\boldsymbol{u}^\alpha$ be the displacement fields of the body Ω^α ($\boldsymbol{u}^\alpha(x) \in \mathbb{R}^d$). We set $\mathbf{u} = (\boldsymbol{u}^1, \boldsymbol{u}^2)$ the displacement field of the two-body system. Hooke's law is assumed for each elastic body, i.e. the stress tensor $\sigma^\alpha(\boldsymbol{v}^\alpha) \in (L^2(\Omega_i))^{d\times d}$ relies on the strain tensor

$$\epsilon(\boldsymbol{v}^\alpha) = \frac{1}{2}(\nabla \boldsymbol{v}^\alpha + (\nabla \boldsymbol{v}^\alpha)^t) \in (L^2(\Omega_i))^{d\times d}$$

through the linear equation

$$\sigma^\alpha(\boldsymbol{v}^\alpha) = 2\mu_\alpha \epsilon(\boldsymbol{v}^\alpha) + \lambda_\alpha \mathrm{tr}(\epsilon(\boldsymbol{v}^\alpha))\mathbb{I}_d$$

where $\lambda_\alpha \geq 0$ and $\mu_\alpha \geq 0$ denote the Lamé constants and $\mathbb{I}_d$ the $d \times d$ identity matrix.

The equilibrium equations are

$$\begin{aligned} -\mathrm{div}\, \sigma^i(\boldsymbol{u}^\alpha) &= \boldsymbol{f}^\alpha \text{ in } \Omega^\alpha, && (2.1)\\ \sigma^i(\boldsymbol{u}^\alpha)\cdot \boldsymbol{n}^\alpha &= \boldsymbol{g}^\alpha \text{ on } \Gamma_N^\alpha, && (2.2)\\ \boldsymbol{u}^\alpha &= 0 \text{ on } \Gamma_D^\alpha, && (2.3) \end{aligned}$$

where $\boldsymbol{n}^\alpha$ stands for the unit outward normal to Ω^α.

2.2 Contact and friction conditions

For a complete formulation it remains to introduce the set of admissible displacement fields and the friction conditions. Let us denote by a subscript H horizontal components and coordinates, e.g.

$$\boldsymbol{x}_H = (x_1, x_2), \quad \boldsymbol{u}_H^\alpha = (u_1^\alpha, u_2^\alpha), \text{ etc.}$$

for $\boldsymbol{x} = (x_1, x_2, x_3)$ and $\boldsymbol{u}^\alpha = (u_1^\alpha, u_2^\alpha, u_3^\alpha)$. Following [19], we assume that Γ_c^1 lies above Γ_c^2 in the reference (undeformed) configuration, and that the contact surfaces are defined parametrically by

$$\begin{aligned} x_3 &= \psi^1(\boldsymbol{x}_H), \quad (\boldsymbol{x}_H, x_3) \in \Gamma_c^1,\\ x_3 &= \psi^2(\boldsymbol{x}_H), \quad (\boldsymbol{x}_H, x_3) \in \Gamma_c^2. \end{aligned}$$

The function ψ^α are assumed to be smooth. Let $\boldsymbol{x}_H^1$ be the coordinate label of a particle on the contact surface Γ_c^1 and $\boldsymbol{x}_H^2$ the unique particle in Γ_c^2 which is the closest to $\boldsymbol{x}_H^1$ in the (current) deformed configuration. Then a displacement field $\mathbf{u} = (\boldsymbol{u}^1, \boldsymbol{u}^2)$ is kinematically admissible if

$$\begin{aligned} \boldsymbol{x}_H^1 + u_H^1(\boldsymbol{x}_H^1, \psi^1(\boldsymbol{x}_H^1)) &= \boldsymbol{x}_H^2 + u_H^2(\boldsymbol{x}_H^2, \psi^2(\boldsymbol{x}_H^2)), && (2.4)\\ \psi^1(\boldsymbol{x}_H^1) + u_3^1(\boldsymbol{x}_H^1, \psi^1(\boldsymbol{x}_H^1)) &\geq \psi^2(\boldsymbol{x}_H^2) + u_3^2(\boldsymbol{x}_H^2, \psi^2(\boldsymbol{x}_H^2)). && (2.5) \end{aligned}$$

To simplify the presentation, we sometimes write $\boldsymbol{u}^\alpha(\boldsymbol{x}_H^\alpha)$ instead of $\boldsymbol{u}^\alpha(\boldsymbol{x}_H^\alpha, \psi^\alpha(\boldsymbol{x}_H^\alpha))$. Assuming infinitesimal deformations we have

$$\begin{aligned} \boldsymbol{u}_H^2(\boldsymbol{x}_H^2) = \boldsymbol{u}_H^2(\boldsymbol{x}_H^2, \psi^2(\boldsymbol{x}_H^2)) &= \boldsymbol{u}_H^2(\boldsymbol{x}_H^1 + \boldsymbol{x}_H^2 - \boldsymbol{x}_H^1, \psi^1(\boldsymbol{x}_H^1) + \psi^2(\boldsymbol{x}_H^2) - \psi^1(\boldsymbol{x}_H^1)) \\ &\approx \boldsymbol{u}_H^2(\boldsymbol{x}_H^1, \psi^1(\boldsymbol{x}_H^1)) \end{aligned} \tag{2.6}$$

by neglecting first order derivative terms, and

$$\psi^2(\boldsymbol{x}_H^2) \approx \psi^2(\boldsymbol{x}_H^1) + \nabla\psi^2(\boldsymbol{x}_H^1)\cdot(\boldsymbol{x}_H^2 - \boldsymbol{x}_H^1) = \psi^2(\boldsymbol{x}_H^1) + \nabla\psi^2(\boldsymbol{x}_H^1)\cdot(\boldsymbol{u}_H^1(\boldsymbol{x}_H^1) - \boldsymbol{u}_H^2(\boldsymbol{x}_H^1)) \tag{2.7}$$

using (2.4). Plugging (2.6) and (2.7) into (2.5), we get

$$\nabla\psi^2(\boldsymbol{x}_H^1)\cdot(\boldsymbol{u}_H^1 - \boldsymbol{u}_H^2) - (u_2^1(\boldsymbol{x}_H^1) - u_2^2(\boldsymbol{x}_H^1)) \le \psi^1(\boldsymbol{x}_H^1) - \psi^2(\boldsymbol{x}_H^1).$$

Setting

$$\begin{aligned} \boldsymbol{n} &= (\nabla\psi^2(\boldsymbol{x}_H^1), -1) \,/\, \sqrt{|\nabla\psi^2(\boldsymbol{x}_H^1)|^2 + 1}, \\ g(\boldsymbol{x}_H^1) &= (\psi^1(\boldsymbol{x}_H^1) - \psi^2(\boldsymbol{x}_H^1)) \,/\, \sqrt{|\nabla\psi^2(\boldsymbol{x}_H^1)|^2 + 1}, \\ [\mathbf{u}_n] &= (\boldsymbol{u}^1(\boldsymbol{x}_H^1) - \boldsymbol{u}^2(\boldsymbol{x}_H^1))\cdot\boldsymbol{n}, \end{aligned}$$

we obtain the contact condition

$$[\mathbf{u}_n] - g \le 0 \quad \text{on } \Gamma_c^1 \text{ and } \Gamma_c^2. \tag{2.8}$$

The vector $\boldsymbol{n}$ stands for the unit outward normal to the boundary Γ_c^1 while g is the normalized initial "gap" between Ω^1 and Ω^2. $[\mathbf{u}_n]$ is the relative normal displacement on the contact surface.

We can identify both surfaces Γ_c^α by their projection Γ_c on the $\boldsymbol{x}_H$ plane so that the contact condition (2.8) can be replaced by

$$[\mathbf{u}_n] - g \le 0 \quad \text{on } \Gamma_c. \tag{2.9}$$

We define the relative tangential displacement on the contact surface Γ_c by

$$[\mathbf{u}_t] = \boldsymbol{u}_t^1 - \boldsymbol{u}_t^2 = \boldsymbol{u}^1 - \boldsymbol{u}^2 - [\mathbf{u}_n]\boldsymbol{n} = [\mathbf{u}] - [\mathbf{u}_n]\boldsymbol{n},$$

where $[\mathbf{u}] = (\boldsymbol{u}^1 - \boldsymbol{u}^2)|_{\Gamma_c}$. Let $\boldsymbol{\sigma}_n$ and $\boldsymbol{\sigma}_t$ denote normal and tangential stress on Γ_c

$$\begin{aligned} \boldsymbol{\sigma}_n &= (\sigma^1(\boldsymbol{u}^1)\boldsymbol{n})\cdot\boldsymbol{n} = -(\sigma^2(\boldsymbol{u}^2)\boldsymbol{n})\cdot\boldsymbol{n}, \\ \boldsymbol{\sigma}_t &= \sigma^\alpha(\boldsymbol{u}^\alpha)\boldsymbol{n} - \boldsymbol{\sigma}_n\boldsymbol{n}. \end{aligned}$$

The contact (nonpenetration) conditions on Γ_c are

$$[\mathbf{u}_n] - g \le 0, \quad \boldsymbol{\sigma}_n \le 0, \quad ([\mathbf{u}_n] - g)\boldsymbol{\sigma}_n = 0, \text{ on } \Gamma_c. \tag{2.10}$$

In addition with the nonpenetration conditions (2.10), the following Tresca friction conditions are prescribed on Γ_c

$$s = \nu_f|\boldsymbol{\sigma}_n|, \qquad |\boldsymbol{\sigma}_t| < s \implies [\mathbf{u}_t] = 0 \text{ on } \Gamma_c, \tag{2.11}$$

$$|\boldsymbol{\sigma}_t| = s \implies \exists \lambda \geq 0,\ [\mathbf{u}_t] = -\lambda \boldsymbol{\sigma}_t \text{ on } \Gamma_c, \tag{2.12}$$

where ν_f stands for the (positive) friction coefficient and s is considered as given.

2.3 Constrained minimization problem

Let us introduce Hilbert spaces of virtual displacements

$$V^\alpha = \left\{ \boldsymbol{v} \in (H^1(\Omega^\alpha))^d \ :\ \boldsymbol{v} = 0 \text{ on } \Gamma_D^\alpha \right\}, \quad \alpha = 1, 2,$$

and we set $\mathbf{V} = V^1 \times V^2$. For $\boldsymbol{u}^\alpha, \boldsymbol{v}^\alpha \in V^\alpha$, we define the bilinear form of virtual works produced by the displacement $\boldsymbol{u}^\alpha$ by

$$a^\alpha(\boldsymbol{u}^\alpha, \boldsymbol{v}^\alpha) = \int_{\Omega^\alpha} \sigma^\alpha(\boldsymbol{u}^\alpha)\epsilon(\boldsymbol{v}^\alpha)dx$$

and the linear form of virtual works due to volume forces and surface traction by

$$\ell^\alpha(\boldsymbol{v}^\alpha) = \int_{\Omega^\alpha} \boldsymbol{f}^\alpha \boldsymbol{v}^\alpha \, dx + \int_{\Gamma_N^\alpha} \boldsymbol{g}^\alpha \boldsymbol{v}^\alpha \, d\Gamma. \tag{2.13}$$

For each body, we define the total potential energy functional J^α by

$$J^\alpha(\boldsymbol{v}^\alpha) = \frac{1}{2} a^\alpha(\boldsymbol{v}^\alpha, \boldsymbol{v}^\alpha) - \ell^\alpha(\boldsymbol{v}^\alpha), \quad \forall \boldsymbol{v}^\alpha \in V^\alpha$$

and we set

$$\boldsymbol{J}(\mathbf{v}) = \sum_{\alpha=1}^{2} J^\alpha(\boldsymbol{v}^\alpha), \quad \mathbf{v} \in \mathbf{V}, \tag{2.14}$$

the total potential energy of the two-body system. Assuming that $\text{mes}(\Gamma_D^\alpha) > 0$, the functional $\boldsymbol{J}$ is convex, G-differentiable and coercive on $\mathbf{V}$.

We now introduce the set of kinematically admissible displacement fields

$$K = \left\{ \mathbf{v} = (\boldsymbol{v}^1, \boldsymbol{v}^2) \in \mathbf{V},\ [\boldsymbol{v}_n] - g \leq 0 \text{ on } \Gamma_c \right\}$$

and the friction functional

$$j(\mathbf{v}) = \int_{\Gamma_c} s|\boldsymbol{v}_t^1 - \boldsymbol{v}_t^2| d\Gamma = \int_{\Gamma_c} s|[\mathbf{v}_t]| d\Gamma,$$

where $|\cdot|$ denotes the Euclidean norm. The functional j is continuous and convex but nondifferentiable.

With the above preparations, the unilateral contact problem with Tresca friction can be formulated as the constrained minimization problem

Find $\mathbf{u} \in K$ such that

$$\boldsymbol{J}(\mathbf{u}) + j(\mathbf{u}) \leq \boldsymbol{J}(\mathbf{v}) + j(\mathbf{v}), \quad \forall \mathbf{v} \in K. \tag{2.15}$$

With the assumption $\text{mes}(\Gamma_D^\alpha) > 0$, the functional $\boldsymbol{J} + j$ is strictly convex and coercive, then there exists a unique solution to (2.15).

3 Domain decomposition

In this section we present our domain decomposition method for solving (2.15). To this end, we need to transform the convex minimization problem (2.15) into a suitable saddle-point problem by introducing auxiliary interface unknowns.

3.1 Augmented Lagrangian formulation

Let us introduce auxiliary unknowns $\boldsymbol{q}_c = (q_c^1, q_c^2)$ and $\boldsymbol{q}_f = (q_f^1, q_f^2)$. Following Fortin and Glowinski [12] or Glowinski and Le Tallec [13], we introduce the set

$$C = \left\{ \boldsymbol{q}_c = (q_c^1, q_c^2) \in (L^2(\Gamma_c))^2,\ q_c^1 - q_c^2 - g \leq 0 \text{ on } \Gamma_c \right\}$$

and its characteristic functional $I_C : (L^2(\Gamma_c))^2 \to \mathbb{R} \cup \{+\infty\}$ defined by

$$I_C(\boldsymbol{q}_c) = \begin{cases} 0 & \text{if } \boldsymbol{q}_c \in C \\ +\infty & \text{if } \boldsymbol{q}_c \notin C \end{cases}$$

Setting

$$\mathbf{q} = (\boldsymbol{q}_c, \boldsymbol{q}_f), \quad H_c = (L^2(\Gamma_c))^2, \quad H_f = (L^2(\Gamma_c))^{2(d-1)} \quad \text{and } H = H_c \times H_f,$$

it is clear that (2.15) is equivalent to the following constrained minimization problem

Find $(\mathbf{u}, \mathbf{p}) \in \mathbf{V} \times H$ such that

$$\boldsymbol{J}(\mathbf{u}) + j(\boldsymbol{p}_f) + I_C(\boldsymbol{p}_c) \leq J(\mathbf{v}) + j(\boldsymbol{q}_f) + I_C(\boldsymbol{q}_c) \quad \forall (\mathbf{v}, \mathbf{q}) \in \mathbf{V} \times H, \tag{3.1}$$

$$\boldsymbol{u}_n^\alpha - p_c^\alpha = 0 \text{ on } \Gamma_c,\ \alpha = 1, 2, \tag{3.2}$$

$$\boldsymbol{u}_t^\alpha - p_f^\alpha = 0 \text{ on } \Gamma_c,\ \alpha = 1, 2. \tag{3.3}$$

To equations (3.1)-(3.3) we associate the augmented Lagrangian functional $\mathscr{L}_r$ defined on $\mathbf{V} \times H \times H$ by

$$\begin{aligned} \mathscr{L}_r(\mathbf{v}, \mathbf{q}; \boldsymbol{\mu}) &= \boldsymbol{J}(\boldsymbol{v}) + j(\boldsymbol{q}_f) + I_C(\boldsymbol{q}_c) + \sum_{\alpha=1}^{2} \left[(\mu_c^\alpha, \boldsymbol{v}_n^\alpha - q_c^\alpha)_{\Gamma_c} + (\mu_f^\alpha, \boldsymbol{v}_t^\alpha - q_f^\alpha)_{\Gamma_c} \right] \\ &+ \frac{r}{2} \sum_{\alpha=1}^{2} \left(\| \boldsymbol{v}_n^\alpha - q_c^\alpha \|_{0,\Gamma_c}^2 + \| \boldsymbol{v}_t^\alpha - q_f^\alpha \|_{0,\Gamma_c}^2 \right), \end{aligned} \tag{3.4}$$

where $r > 0$ is the penalty parameter and $\boldsymbol{\mu} = (\boldsymbol{\mu}_c, \boldsymbol{\mu}_f)$. The corresponding saddle-point problem is

Find $((\mathbf{u}, \mathbf{p}), \boldsymbol{\lambda}) \in \mathbf{V} \times H \times H$ such that

$$\mathscr{L}_r(\mathbf{u}, \mathbf{p}; \boldsymbol{\mu}) \leq \mathscr{L}_r(\mathbf{v}, \mathbf{q}; \boldsymbol{\mu}) \leq \mathscr{L}_r(\mathbf{v}, \mathbf{q}; \boldsymbol{\lambda}), \quad \forall((\mathbf{v}, \mathbf{q}), \boldsymbol{\mu}) \in \mathbf{V} \times H \times H, \tag{3.5}$$

where we have set $\boldsymbol{\lambda} = (\boldsymbol{\lambda}_c, \boldsymbol{\lambda}_f)$.

3.2 Uzawa block relaxation method

A saddle-point of $\mathscr{L}_r$ can be determined by a standard Uzawa method for augmented Lagrangian, see e.g. [3, 4]. The main difficulty with the standard Uzawa method is the coupling of subdomains and unknowns $\boldsymbol{u}$ and $\mathbf{p}$. By introducing auxiliary unknowns, $\boldsymbol{p}_c$ and $\boldsymbol{p}_f$, we have implicitly split the problem in a "linear part" (subproblem in $\mathbf{u}$) and a "nonlinear part" (subproblem in $\mathbf{p}$). Furthermore, the displacement fields on subdomains Ω^1 and Ω^2 are now linked only through the auxiliary unknowns. To take advantage of these properties, a quite natural method consists of using a Uzawa block relaxation method.

Uzawa block relaxation methods have been used in nonlinear mechanics for operator splitting and domain decomposition methods [12, 13, 21]. Applying a Uzawa block relaxation (UBR) method to the saddle-point problem (3.5), we obtain the following algorithm.

Algorithm UBR

Initialization. $\mathbf{p}^{-1} = (\boldsymbol{p}_c^{-1}, \boldsymbol{p}_f^{-1})$ and $\boldsymbol{\lambda}^0 = (\boldsymbol{\lambda}_c^0, \boldsymbol{\lambda}_f^0)$ are given.

Iteration $k \geq 0$. Compute successively $\mathbf{u}^k = (\boldsymbol{u}^{1,k}, \boldsymbol{u}^{2,k})$, $\mathbf{p}^k = (\boldsymbol{p}_c^k, \boldsymbol{p}_f^k)$ and $\boldsymbol{\lambda}^{k+1} = (\boldsymbol{\lambda}_c^{k+1}, \boldsymbol{\lambda}_f^{k+1})$ as follows.

- Find $\mathbf{u}^k \in \mathbf{V}$ such that

$$\mathscr{L}_r(\mathbf{u}^k, \mathbf{p}^{k-1}; \boldsymbol{\lambda}^k) \leq \mathscr{L}_r(\mathbf{v}, \mathbf{p}^{k-1}; \boldsymbol{\lambda}^k), \quad \forall \mathbf{v} \in \mathbf{V}. \tag{3.6}$$

- Find $\mathbf{p}^k = (\boldsymbol{p}_c^k, \boldsymbol{p}_f^k) \in H$ such that

$$\mathscr{L}_r(\mathbf{u}^k, \mathbf{p}^k; \boldsymbol{\lambda}^k) \leq \mathscr{L}_r(\mathbf{u}^k, \mathbf{q}; \boldsymbol{\lambda}^k), \quad \forall \mathbf{q} \in H. \tag{3.7}$$

- Update the Lagrange multipliers

$$\begin{aligned} \lambda_c^{\alpha,k+1} &= \lambda_c^{\alpha,k} + r(\boldsymbol{u}_n^{\alpha,k} - p_c^{\alpha,k}), \ \alpha = 1, 2, \\ \lambda_f^{\alpha,k+1} &= \lambda_f^{\alpha,k} + r(\boldsymbol{u}_t^{\alpha,k} - p_f^{\alpha,k}), \ \alpha = 1, 2. \end{aligned}$$

We detail the above algorithm in the next subsections.

3.3 Solution of subproblem (3.6)

Since the functional $\mathbf{v} \mapsto \mathscr{L}_r(\mathbf{v}, \mathbf{p}^{k-1}, \boldsymbol{\lambda}^k)$ is convex and Gâteau-differentiable on $\mathbf{V}$, the solution of (3.6) can be characterized by the Euler-Lagrange equation

$$\frac{\partial}{\partial \mathbf{v}} \mathscr{L}_r(\mathbf{u}^k, \mathbf{p}_c^{k-1}, \boldsymbol{\lambda}_c^k) \cdot \mathbf{v} = 0, \quad \forall \mathbf{v} \in \mathbf{V}.$$

A straightforward calculation yields

Find $\boldsymbol{u}^{\alpha,k} \in V^\alpha$ such that

$$\begin{aligned} a^\alpha(\boldsymbol{u}^{\alpha,k}, \boldsymbol{v}^\alpha) + r(\boldsymbol{u}_n^{\alpha,k}, \boldsymbol{v}_n^\alpha)_{\Gamma_c} &+ r(\boldsymbol{u}_t^{\alpha,k}, \boldsymbol{v}_t^\alpha)_{\Gamma_c} = \ell^\alpha(\boldsymbol{v}^\alpha) + (rp_c^{\alpha,k-1} - \lambda_c^{\alpha,k}, \boldsymbol{v}_n^\alpha)_{\Gamma_c} \\ &+ (rp_f^{\alpha,k-1} - \lambda_f^{\alpha,k}, \boldsymbol{v}_t^\alpha)_{\Gamma_c} \quad \forall \boldsymbol{v}^\alpha \in V^\alpha, \alpha = 1, 2. \quad (3.8) \end{aligned}$$

The main property of the Uzawa block relaxation now appears: the linear elasticity problems on each subdomain are now uncoupled.

3.4 Solution of subproblem (3.7)

Note that in (3.7) subproblems in $\boldsymbol{p}_c$ and $\boldsymbol{p}_f$ are uncoupled. Consequently, we can minimize the functional $\mathbf{q} = (\boldsymbol{q}_c, \boldsymbol{q}_f) \mapsto \mathscr{L}_r(\mathbf{u}^k, \mathbf{q}, \boldsymbol{\lambda}^k)$ separately in $\boldsymbol{q}_c$ and $\boldsymbol{q}_f$.

3.4.1 Nonpenetration subproblem

Over the nonpenetration constraints set C the functional $\boldsymbol{q}_c \mapsto \mathscr{L}_r(\mathbf{u}^k, \boldsymbol{q}_c, \boldsymbol{\lambda}^k)$ can be simplified

$$\Phi_c(\boldsymbol{q}_c) := \mathscr{L}_r(\mathbf{u}^k, \boldsymbol{q}_c, \boldsymbol{q}_f, \boldsymbol{\lambda}^k) = \sum_{\alpha=1}^{2} \left[\frac{r}{2} \parallel q_c^\alpha \parallel_{0,\Gamma_c}^2 - (\lambda_c^{\alpha,k} + r\boldsymbol{u}_n^{\alpha,k}, p_c^\alpha)_{\Gamma_c} \right] + \beta,$$

where β is a constant which does not count in the minimization. The functional Φ_c is convex and coercive over the convex set C. The infimum $\boldsymbol{p}_c^k$ of the functional Φ_c must satisfied the Kuhn-Tucker conditions

$$\begin{aligned} \sum_{\alpha=1}^{2} \left[r(p_c^{\alpha,k}, q_c^\alpha)_{\Gamma_c} - (\lambda_c^{\alpha,k} + r\boldsymbol{u}_n^{\alpha,k}, q_c^\alpha)_{\Gamma_c} \right] + (\gamma^k, q_c^1 - q_c^2)_{\Gamma_c} &= 0, \quad \forall (q_c^1, q_c^2), \quad (3.9) \\ (\gamma^k, p_c^{1,k} - p_c^{2,k} - g)_{\Gamma_c} &= 0, \quad (3.10) \end{aligned}$$

where $\gamma^k \geq 0$ is referred as a Lagrange (Kuhn-Tucker) multiplier for the constraints set C (see e.g. [17, 25]). From (3.9) we deduce that

$$p_c^{\alpha,k} = \boldsymbol{u}_n^{\alpha,k} + \frac{1}{r} \left(\lambda_c^{\alpha,k} + (-1)^\alpha \gamma^k \right), \quad \alpha = 1, 2. \quad (3.11)$$

Substituting (3.11) into (3.10), we obtain

$$\left(\gamma^k, \frac{1}{r} \left([\boldsymbol{\lambda}^k] + r[\mathbf{u}_n^k] - 2\gamma^k \right) - g \right)_{\Gamma_c} = 0,$$

where we have set $[\boldsymbol{\lambda}_c^k] = \lambda_c^{1,k} - \lambda_c^{2,k}$. From (3.10) if $\gamma^k > 0$, we must have

$$\frac{1}{r}\left([\boldsymbol{\lambda}_c^k] + r[\mathbf{u}_n^k] - 2\gamma^k\right) - g = 0$$

implying that

$$\gamma^k = \frac{1}{2}\left([\boldsymbol{\lambda}_c^k] + r([\mathbf{u}_n^k] - g)\right).$$

Since $\gamma^k \geq 0$, we set

$$\gamma^k = \frac{1}{2}\left([\boldsymbol{\lambda}_c^k] + r([\mathbf{u}_n^k] - g)\right)^+ := \max\left\{0, \frac{1}{2}\left([\boldsymbol{\lambda}_c^k] + r([\mathbf{u}_n^k] - g)\right)\right\}. \tag{3.12}$$

Substituting (3.12) into (3.11), we deduce the auxiliary contact unknowns

$$p_c^{\alpha,k} = \boldsymbol{u}_n^{\alpha,k} + \frac{1}{r}\lambda_c^{\alpha,k} + \frac{(-1)^\alpha}{2r}\left([\boldsymbol{\lambda}_c^k] + r([\mathbf{u}_n^k] - g)\right)^+, \quad \alpha = 1, 2. \tag{3.13}$$

We easily verify that

- if $\gamma^k > 0$, then $p_c^{1,k} - p_c^{2,k} - g = 0$;
- if $\gamma^k = 0$, then $p_c^{1,k} - p_c^{2,k} - g \leq 0$.

3.4.2 Friction subproblem

We now compute the solution of the Tresca friction subproblem. The functional $\boldsymbol{q}_f \mapsto \mathscr{L}_r(\mathbf{u}^k, \boldsymbol{q}_f, \boldsymbol{\lambda}^k)$ can be rewritten as

$$\Phi_f(\boldsymbol{q}_f) := \frac{r}{2} \parallel \boldsymbol{q}_f \parallel_{0,\Gamma_c}^2 - (\mathbf{b}^k, \boldsymbol{q}_f)_{\Gamma_c} + \int_{\Gamma_c} s|q_f^1 - q_f^2| d\Gamma + \beta,$$

where, for clarity, we have set

$$b^{\alpha,k} = \lambda_f^{\alpha,k} + r\boldsymbol{u}_t^{\alpha,k}, \quad \alpha = 1, 2, \quad \mathbf{b}^k = (b^{1,k}, b^{2,k}) \tag{3.14}$$

and β a constant which does not count in the minimization. The friction subproblem is therefore

Find $\boldsymbol{p}_f \in H_f$ such that

$$\Phi_f(\boldsymbol{p}_f) \leq \Phi_f(\boldsymbol{q}_f), \quad \forall \boldsymbol{q}_f \in H_f. \tag{3.15}$$

Let $\mathcal{F} : X = H_f \to \mathbb{R}$ and $\mathcal{G} : Y = (L^2(\Gamma_c))^{d-1} \to \mathbb{R}$ be defined by

$$\mathcal{F}(\boldsymbol{q}_f) = \frac{r}{2} \parallel \boldsymbol{q}_f \parallel_{0,\Gamma_c}^2 - (\mathbf{b}^k, \boldsymbol{q}_f)_{\Gamma_c} = \sum_{\alpha=1}^{2}\left(\frac{r}{2} \parallel q_f^\alpha \parallel_{0,\Gamma_c} + (b^{\alpha,k}, q_f^\alpha)_{\Gamma_c}\right), \tag{3.16}$$

$$\mathcal{G}(y) = \int_{\Gamma_c} s|y| d\Gamma. \tag{3.17}$$

The functionals $\mathcal{F}$ and $\mathcal{G}$ are convex and continuous. We introduce the bounded linear operator $\Lambda \in \mathcal{L}(X, Y)$ defined by

$$\Lambda \boldsymbol{q}_f = q_f^1 - q_f^2 = [\boldsymbol{q}_f]$$

so that,

$$\mathcal{G}(\Lambda \boldsymbol{q}_f) = \int_{\Gamma_c} s|[\boldsymbol{q}_f]| d\Gamma.$$

The minimization problem (3.15) becomes

$$(P) \quad \inf_{\boldsymbol{q}_f \in X} \mathcal{F}(\boldsymbol{q}_f) + \mathcal{G}(\Lambda \boldsymbol{q}_f).$$

The Fenchel dual problem of (P) is

$$(P^*) \quad \sup_{y^* \in Y^*} -\mathcal{F}(-\Lambda^* y^*) - \mathcal{G}(y^*)$$

where $\Lambda^* \in \mathcal{L}(Y^*, X^*)$ is the adjoint of Λ and $\mathcal{F}^* : X^* = X \to \mathbb{R} \cup \{\infty\}$, $\mathcal{G}^* : Y^* = Y \to \mathbb{R} \cup \{\infty\}$ denote the Fenchel convex conjugate functionals (see e.g. [10]) of $\mathcal{F}$ and $\mathcal{G}$, respectively. It is easy to see that $\mathcal{F}$ and $\mathcal{G}$ satisfy the conditions of the Fenchel duality theorem [10, p. 59] and thus it follows that no duality gap occurs. Then the solutions $\boldsymbol{p}_f$ and $\bar{y}^*$ of (P) and (P^*) satisfy the extremality condition [10, p. 53]

$$-\Lambda^* \bar{y}^* \in \partial \mathcal{F}(\boldsymbol{p}_f) \tag{3.18}$$

where ∂ denotes the subdifferential.

Let $\boldsymbol{q}_f^* \in X^*$ be given. From the definition of the Fenchel convex conjugate we have

$$\begin{aligned} \mathcal{F}^*(\boldsymbol{q}_f^*) &= \sup_{\boldsymbol{q}_f \in X} (\boldsymbol{q}_f^*, \boldsymbol{q}_f)_{\Gamma_c} - \frac{r}{2} \parallel \boldsymbol{q}_f \parallel_{0,\Gamma_c}^2 + (\mathbf{b}^k, \boldsymbol{q}_f)_{\Gamma_c} \\ &= \sup_{\boldsymbol{q}_f \in X} (\boldsymbol{q}_f^* + \mathbf{b}^k, \boldsymbol{q}_f)_{\Gamma_c} - \frac{r}{2} \parallel \boldsymbol{q}_f \parallel_{0,\Gamma_c}^2 \\ &= \frac{1}{2r} \parallel \boldsymbol{q}_f^* + \mathbf{b}^k \parallel_{0,\Gamma_c}^2 = \frac{1}{2r} \sum_{\alpha=1}^{2} \parallel q_f^{\alpha,*} + b^{\alpha,k} \parallel_{0,\Gamma_c}^2 . \end{aligned} \tag{3.19}$$

For $y^* \in Y^*$, the Fenchel convex conjugate functional of $\mathcal{G}$ is

$$\mathcal{G}^*(y^*) = \sup_{y \in Y} (y^*, y)_{\Gamma_c} - \int_{\Gamma_c} s|y| d\Gamma = \begin{cases} 0 & \text{if } |y^*| \le s, \\ +\infty & \text{if } |y^*| \ge s. \end{cases} \tag{3.20}$$

From (3.19), we have

$$\mathcal{F}^*(-\Lambda^* y^*) = \mathcal{F}^*(-y^*, y^*) = \frac{1}{2r} \left(\parallel b^{1,k} - y^* \parallel_{0,\Gamma_c}^2 + \parallel b^{2,k} + y^* \parallel_{0,\Gamma_c}^2 \right).$$

Then the dual problem (P^*) becomes

$$\sup_{y^*\in Y^*} -\mathcal{F}(-\Lambda^* y^*) - \mathcal{G}(y^*) = \sup_{|y^*|\le s} -\frac{1}{2r}\left(\| b^{1,k} - y^* \|^2_{0,\Gamma_c} + \| b^{2,k} + y^* \|^2_{0,\Gamma_c} \right).$$

The unique solution of this problem is

$$\bar{y}^* = \begin{cases} \frac{1}{2}[\mathbf{b}^k] & \text{if } |[\mathbf{b}]| \le 2s, \\ s\frac{[\mathbf{b}^k]}{|[\mathbf{b}^k]|} & \text{if } |[\mathbf{b}]| \ge 2s. \end{cases} \tag{3.21}$$

To compute the primal solution $\boldsymbol{p}_f$ from the dual solution $\bar{y}^*$ given by (3.21), we use (3.19) and the extremality condition (3.18) ($\mathcal{F}^*$ being a differentiable functional)

$$\nabla\mathcal{F}(\boldsymbol{p}_f) = -\Lambda^*\bar{y}^* = \begin{pmatrix} -\bar{y}^* \\ \bar{y}^* \end{pmatrix}$$

A straightforward calculation yields, for $\alpha = 1, 2$,

$$p_f^{\alpha,k} = \frac{1}{2r}(b^{1,k} + b^{2,k}), \quad \text{if } |[\mathbf{b}^k]| \le 2s, \tag{3.22}$$

$$p_f^{\alpha,k} = \frac{1}{r}b^{\alpha,k} + \frac{(-1)^\alpha}{r} s\frac{[\mathbf{b}^k]}{|[\mathbf{b}^k]|}, \quad \text{if } |[\mathbf{b}^k]| \ge 2s. \tag{3.23}$$

Substituting (3.14) into (3.22)-(3.23), we obtain the solution of the Tresca friction subproblem

$$p_f^{\alpha,k} = \begin{cases} \dfrac{1}{2r}\displaystyle\sum_{\alpha=1}^{2}\left(\lambda_f^{\alpha,k} + r\boldsymbol{u}_t^{\alpha,k}\right) & \text{if } |[\boldsymbol{\lambda}_f^k] + r[\mathbf{u}_t]| \le 2s, \\ \boldsymbol{u}_t^{\alpha,k} + \dfrac{1}{r}\lambda_f^{\alpha,k} + \dfrac{(-1)^\alpha s}{r}\dfrac{[\boldsymbol{\lambda}_f^k] + r[\mathbf{u}_t^k]}{|[\boldsymbol{\lambda}_f^k] + r[\mathbf{u}_t^k]|} & \text{if } |[\boldsymbol{\lambda}^k] + r[\mathbf{u}_t^k]| \ge 2s \end{cases}, \quad \alpha = 1, 2.$$

3.5 Domain decomposition algorithm

With the results of the previous subsections, we can now present our Uzawa block relaxation domain decomposition algorithm.

Algorithm UBR-DDM

Initialization. $\mathbf{p}^{-1} = (\boldsymbol{p}_c^{-1}, \boldsymbol{p}_f^{-1})$ and $\boldsymbol{\lambda}^0 = (\boldsymbol{\lambda}_c^0, \boldsymbol{\lambda}_f^0)$ are given.

Iteration $k \ge 0$. Compute successively $\boldsymbol{u}^k$, $\mathbf{p}^k$ and $\boldsymbol{\lambda}^{k+1}$ as follows

- Find $\boldsymbol{u}^{\alpha,k} \in V^\alpha$ such that

$$\begin{aligned} a^\alpha(\boldsymbol{u}^{\alpha,k}, \boldsymbol{v}^\alpha) + r(\boldsymbol{u}_n^{\alpha,k}, \boldsymbol{v}_n^\alpha)_{\Gamma_c} &+ r(\boldsymbol{u}_t^{\alpha,k}, \boldsymbol{v}_t^\alpha)_{\Gamma_c} = \ell^\alpha(\boldsymbol{v}^\alpha) + (rp_c^{\alpha,k-1} - \lambda_c^{\alpha,k}, \boldsymbol{v}_n^\alpha)_{\Gamma_c} \\ &+ (rp_f^{\alpha,k-1} - \lambda_f^{\alpha,k}, \boldsymbol{v}_t^\alpha)_{\Gamma_c} \quad \forall \boldsymbol{v}^\alpha \in V^\alpha, \alpha = 1, 2. \end{aligned}$$

- Compute the auxiliary interface unknowns ($\alpha = 1, 2$)

$$p_c^{\alpha,k} = \boldsymbol{u}_n^{\alpha,k} + \frac{1}{r}\lambda_c^{\alpha,k} + \frac{(-1)^\alpha}{2r}\left([\boldsymbol{\lambda}_c^k] + r([\mathbf{u}_n^k] - g)\right)^+,$$

$$p_f^{\alpha,k} = \begin{cases} \dfrac{1}{2r}\left(\lambda_f^{1,k} + \lambda_f^{2,k} + r(\boldsymbol{u}_t^{1,k} + \boldsymbol{u}_t^{2,k})\right) & \text{if } |[\boldsymbol{\lambda}^k] + r[\mathbf{u}_t]| \le 2s, \\ \boldsymbol{u}_t^{\alpha,k} + \dfrac{1}{r}\lambda_f^{\alpha,k} + \dfrac{(-1)^\alpha s}{r}\dfrac{[\boldsymbol{\lambda}^k] + r[\mathbf{u}_t^k]}{|[\boldsymbol{\lambda}^k] + r[\mathbf{u}_t^k]|} & \text{if } |[\boldsymbol{\lambda}^k] + r[\mathbf{u}_t^k]| \ge 2s \end{cases}.$$

- Update the Lagrange multipliers

$$\lambda_c^{\alpha,k+1} = \lambda_c^{\alpha,k} + r(\boldsymbol{u}_n^{\alpha,k} - p_c^{\alpha,k}),\ \alpha = 1, 2,$$
$$\lambda_f^{\alpha,k+1} = \lambda_f^{\alpha,k} + r(\boldsymbol{u}_t^{\alpha,k} - p_f^{\alpha,k}),\ \alpha = 1, 2.$$

We iterate until the relative error on $\boldsymbol{u}^k$, $\boldsymbol{p}_c^k$ and $\boldsymbol{p}_f^k$ becomes sufficiently small. The parallelizability of the above algorithm is obvious since, in every iteration, we solve in parallel two linear elasticity subproblems. Furthermore, the left-hand sides of the linear elasticity subproblems do not change during the iterative process implying the saving of computational cost due to matrix factorizations.

4 Convergence results

We first rewrite the constrained optimization problem (2.15) in a standard form. To this end we set

$$G(\mathbf{v}) = \boldsymbol{J}(\mathbf{v}), \quad F(\mathbf{q}) = I_C(\boldsymbol{q}_c) + j(\boldsymbol{q}_f)$$

and we introduce the linear and continuous operator B, from $\mathbf{V} \to L^2(\Gamma_c) \times L^2_T(\Gamma_c)$, defined by

$$B\mathbf{v} = \begin{pmatrix} [\mathbf{v}_n] - g \\ [\mathbf{v}_t] \end{pmatrix},$$

where

$$L^2_T(\Gamma_c) = \left\{\boldsymbol{v} \in (L^2(\Gamma_c))^d \mid \boldsymbol{v}_n = 0\right\}.$$

We observe that (2.15) is equivalent to

Find $\mathbf{u} \in \mathbf{V}$ such that

$$G(\mathbf{u}) + F(B\mathbf{u}) \le G(\mathbf{v}) + F(B\mathbf{v}), \quad \forall \mathbf{v} \in \mathbf{V}.$$

The functional G is convex, proper and lower semi-continuous while F is strictly convex and continuous. Furthermore, G is uniformly convex on the bounded sets of $\mathbf{V}$. Algorithm UBR-DDM is therefore equivalent to the operator-splitting standard algorithm ALG2 described, e.g., in [13, ch. 3] or [12, ch. 3]. We have the following convergence theorem, see e.g. [13, ch. 3, theorem 4.2].

Theorem 4.1 (Convergence). *The sequence* $(\mathbf{u}^k, \boldsymbol{p}^k, \boldsymbol{\lambda}^k)$ *generated in Algorithm UBR-DDM is such that*

$$\mathbf{u}^k \to \mathbf{u} \text{ in } \mathbf{V}, \quad \mathbf{p}^k \to \mathbf{p} \text{ in } H, \quad \boldsymbol{\lambda}^k \rightharpoonup \boldsymbol{\lambda} \text{ in } H,$$

$(\mathbf{u}, \mathbf{p}, \boldsymbol{\lambda})$ *being a saddle-point of* $\mathscr{L}_r$.

We now investigate how to recover the normal and tangential stress at the end of the the domain decomposition algorithm.

Corollary 4.2 (Normal stress). *The contact pressure is given by* $\boldsymbol{\sigma}_n = -[\boldsymbol{\lambda}_c]/2$.

Proof. Since the Lagrange multiplier $\bar{\lambda}_c$ associated with the contact condition (2.9) is the negative stress in the normal direction, we deduce from (3.12) that $\gamma^k \rightharpoonup [\boldsymbol{\lambda}_c]/2 = \bar{\lambda}_c$. □

Corollary 4.3 (Tangential stress). *The friction stress is given by* $\boldsymbol{\sigma}_t = -[\boldsymbol{\lambda}_f]/2$.

Proof. As in the case of the contact condition, the Lagrange multiplier $\bar{\lambda}_f$, associated with the non-differentiability of the friction functional j, has a mechanical interpretation

$$\bar{\lambda}_f = -\boldsymbol{\sigma}_t.$$

Since $s \in L^2(\Gamma_c)$, the nondifferentiability constraint on $\bar{\lambda}_f$ can be simplified to

$$|\bar{\lambda}_f| \leq s, \text{ a.e. on } \Gamma_c. \tag{4.1}$$

Note that from Lagrange multipliers update formula, we have

$$[\boldsymbol{\lambda}_f^{k+1}] = [\boldsymbol{\lambda}_f^k] + r([\mathbf{u}_t^k] - [\mathbf{p}_f^k]). \tag{4.2}$$

If $|[\boldsymbol{\lambda}_f^k] + r[\mathbf{u}_t]| \leq 2s$, then $[\boldsymbol{p}_f] = 0$ and

$$[\boldsymbol{\lambda}_f^{k+1}] = [\boldsymbol{\lambda}_f^{k+1}] + r[\mathbf{u}_t^k].$$

We deduce that $[\boldsymbol{\lambda}_f^{k+1}]/2$ verifies (4.1).

If $|[\boldsymbol{\lambda}_f^k] + r[\mathbf{u}_t]| \geq 2s$, then

$$[\mathbf{p}_f^k] = [\mathbf{u}_t^k] + \frac{1}{r}[\boldsymbol{\lambda}_f^k] - \frac{2s}{r}\frac{[\boldsymbol{\lambda}_f^k] + r[\mathbf{u}_t^k]}{|[\boldsymbol{\lambda}_f^k] + r[\mathbf{u}_t^k]|},$$

that is

$$r([\mathbf{u}_t^k] - [\mathbf{p}_f^k]) = -[\boldsymbol{\lambda}_f^k] + 2s\frac{[\boldsymbol{\lambda}_f^k] + r[\mathbf{u}_t^k]}{|[\boldsymbol{\lambda}_f^k] + r[\mathbf{u}_t^k]|}. \tag{4.3}$$

Substituting (4.3) into (4.2), we get

$$[\boldsymbol{\lambda}_f^{k+1}] = 2s\frac{[\boldsymbol{\lambda}_f^k] + r[\mathbf{u}_t^k]}{|[\boldsymbol{\lambda}_f^k] + r[\mathbf{u}_t^k]|}$$

and we deduce that (4.1) is valid for $[\boldsymbol{\lambda}_f^{k+1}]/2$, for all $k \geq 0$.

Since the set $\{\mu \in L^2(\Gamma_c) \ : \ |\mu| \leq s\}$ is convex, then the weak limit of the sequence $\{[\boldsymbol{\lambda}_f^k]/2\}$, i.e. $[\boldsymbol{\lambda}_f]/2$, satisfies the inequality (4.1). Finally we conclude that, $[\boldsymbol{\lambda}_f^k]/2 \rightharpoonup [\boldsymbol{\lambda}_f]/2 = \bar{\lambda}_f$. □

5 Numerical experiments

Algorithms UBR-DDM was implemented in Matlab 7 using piecewise linear finite element and vectorized codes [22]. The test problems used are designed to illustrate the behavior of the algorithm more than to model contact actual phenomena. Nondimensionalized units are used and the deformed configurations are plotted with a magnification of the displacement.

Since the matrices of the linear elasticity subproblems (3.8) do not change during the iterative process, a Cholesky factorization is performed once and for all in the initialization step. Then, in the rest of the iterative process, the solution of the linear elasticity subproblems reduces to foreward/backward substitutions. To reduce fill-in, the Cholesky factorization is done after columns and rows permutation with the Matlab function `symamd`.

In all numerical experiments reproted in this section, the stopping criterion is

$$\| \mathbf{u}_h^k - \mathbf{u}_h^{k-1} \|_{0,\Omega}^2 + \| \mathbf{p}_h^k - \mathbf{p}_h^{k-1} \|_{0,\Gamma_c}^2 < 10^{-12} \left(\| \mathbf{u}_h^k \|_{0,\Omega}^2 + \| \mathbf{p}_h^k \|_{0,\Gamma_c}^2 \right).$$

The penalty parameter is $r = \min(E^1, E^2)$ in § 5.1 and $r = \max(E^1, E^2)$ in § 5.2.

5.1 Example 1: Hertz problem

To illustrate the numerical behavior of Algorithm UBR-DDM, a Hertz contact problem is considered, see e.g. [19]. The problem consist of an infinitely long elastic cylinder Ω^1 (radius $R = 8$, $E^1 = 2 \times 10^3$, $\nu^1 = 0.3$) resting on an elastic foundation Ω^2 ($E^1 = 10^4$, $\nu^1 = 0.4$). The cylinder is subjected to a uniform load, along its top, of intensity $P = 1600$. The friction coefficient is $\nu_f = 0.6$. Taking into account the symmetry of the problem, we restrict our study to the subdomains

$$\begin{aligned} \Omega_1 &= \left\{ (x_1, x_2) \mid 0 \le x_1 \le 8,\ R - \sqrt{R^2 - x_1^2} \le x_2 \le 8 \right\}, \\ \Omega_1 &= \{ (x_1, x_2) \mid 0 \le x_1 \le 8,\ -4 \le x_2 \le 0 \} \end{aligned}$$

with suitable boundary conditions. The contact surfaces are

$$\Gamma_c^1 = \left\{ (x_1, x_2) \mid 0 \le x_1 \le 4,\ x_2 = R - \sqrt{R^2 - x_1^2} \right\} \text{ and } \Gamma_c^2 = (0,\ 4) \times \{0\}$$

Their common projection is $\Gamma_c = (0,\ 4) \times \{0\}$ and the normalized gap is $g(x_1) = x_2$. For the frictionless problem we will compare our numerical contact pressure with the analytical contact pressure due to Hertz (see e.g. [14, 18]). For the problem with Tresca friction, we set $s(x) = \nu_f |p(x)|$, where p is the analytical contact pressure.

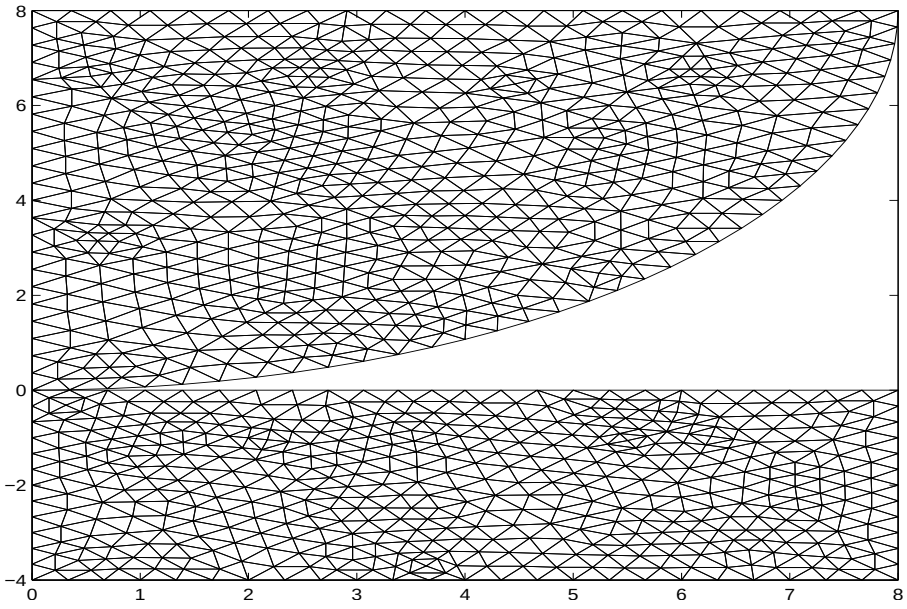

Figure 1: Mesh sample for a Hertz contact problem

5.1.1 Matching meshes

We first study the Hertz problem with the node-on-node contact condition. In this case, it is necessary that the nodes opposite to one another on Γ_c^1 and Γ_c^2 have the same x_1 coordinate. The subdomains Ω^1 and Ω^2 are discretized using nonuniform meshes consisting of 649 and 489 nodes, respectively, with 13 nodes on Γ_c, as shown in Figure 1.

Applying to this problem, Algorithm UBR-DDM stops after 40 iterations in the frictionless case and 32 in the case with friction. Figure 2 shows the deformed configuration in frictionless case. The grey tones visualize the Von Mises effective stress distribution in Ω^1 and Ω^2. In Figures 3-4 we compare the numerical (interface) stress, obtained with Algorithm UBR-DDM, and the analytical Hertz solution. We observe a quite good agreement with the Hertz solution even though a coarse mesh is used.

To study the scalability of the algorithm, the initial mesh is uniformly refined successively to produce meshes with 2513/1881, 9889/7377, 39233/29217 nodes on Ω^1/Ω^2 with 25, 49 and 97 nodes on Γ_c. Table 1 shows the behavior of the algorithm. We can notice that the number of iterations is virtually independent of the mesh size, i.e. the algorithm is scalable.

5.1.2 Nonmatching meshes

In the case the meshes do not match on Γ_c, we have two meshes Γ_{ch_1} and Γ_{ch_2} for Γ_c. The mesh Γ_{ch_1} (resp. Γ_{ch_2}) is induced by Ω_h^1 (resp. Ω_h^2). The contact condition (2.9) is then taken into account using a node-to-segment condition [19, 29, 30, 31]. We use projection procedures to compute the auxiliary interface unknowns while the rest of the

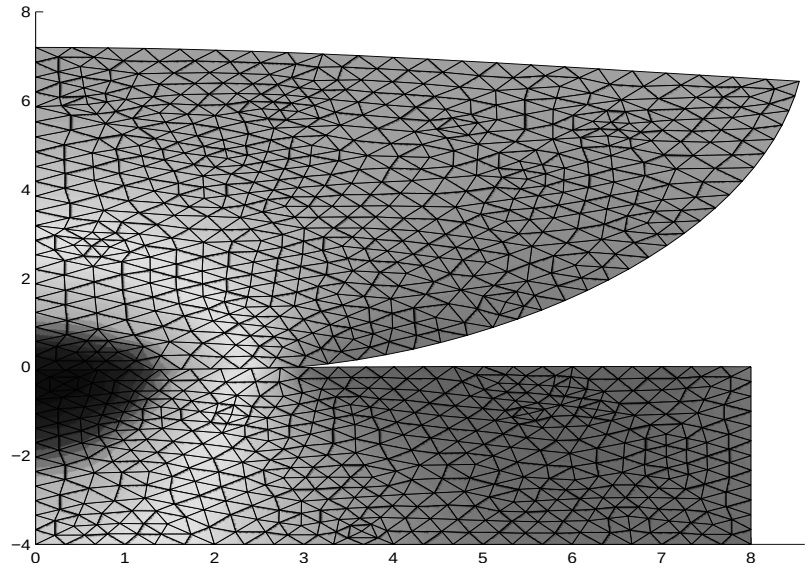

Figure 2: Deformed configuration and Von Mises effective stress for a Hertz problem without friction

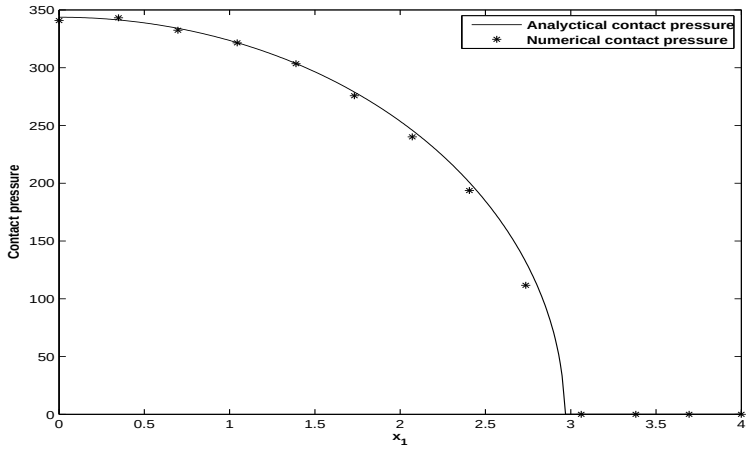

Figure 3: Contact pressure distribution for a Hertz problem without friction

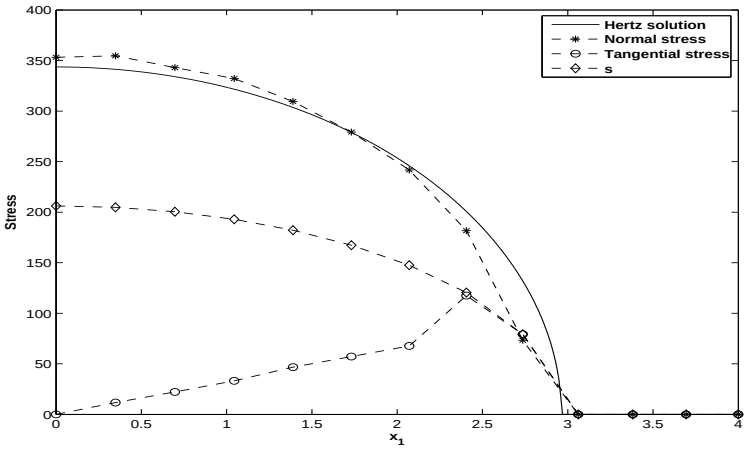

Figure 4: Stress distributions for a Hertz problem with Tresca friction

	Number of Iterations	
Interface nodes	Frictionless case	Friction case
13	40	32
25	48	42
49	48	45
97	46	42

Table 1: Performances of Algorithm UBR-DDM on Hertz problem with matching meshes

algorithm remains unchanged. For instance, for the auxiliary variable $\boldsymbol{p}_c$, we replace (3.13) by the following formulas

$$\begin{aligned} p_{ch}^{1,k} &= u_{nh}^{1,k} + \frac{1}{r}\lambda_{ch}^{1,k} - \frac{1}{2r}\left(\lambda_{ch}^{1,k} - \pi_1(\lambda_{ch}^{2,k}) + r(u_{nh}^{1,k} - \pi_1(u_{nh}^{2,k}) - g)\right)^+ \\ p_{ch}^{2,k} &= u_{nh}^{2,k} + \frac{1}{r}\lambda_{ch}^{2,k} - \frac{1}{2r}\left(\pi_2(\lambda_{ch}^{1,k}) - \lambda_{ch}^{2,k} + r(\pi_2(u_{nh}^{1,k}) - u_{nh}^{2,k} - g)\right)^+ \end{aligned}$$

where $\pi_\alpha(\cdot)$ stands for the projection onto Γ_{ch_α}. We then obtain a symmetric node-to-segment contact condition. The so-called "locking" phenomenon (see e.g. [19]) is avoided since the node-on-segment condition is applied in a symmetrical way.

For the numerical behavior of the algorithm, we use a sequence of nonmatching meshes with 524/253, 2023/961, 7949/3745 and 31513/14785 nodes on Ω_h^1/Ω_h^2; and 11/9, 21/17, 41/33 and 81/65 nodes on $\Gamma_{ch_1}/\Gamma_{ch_2}$. Figures 5-6 show the undeformed and deformed configurations with the coarse mesh. Figures 7-8 depict the stress distributions on Γ_c. The results are in accordance with the ones of the node-to-node contact condition. We report in Table 2 the performance of the algorithm with nonmatching meshes. We can notice that the number of iterations required for convergence is virtually independent of the mesh size.

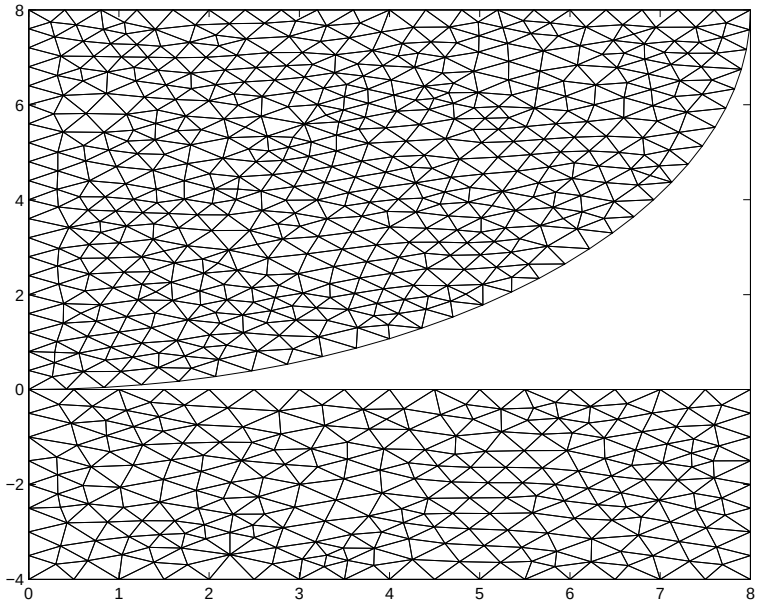

Figure 5: Hertz contact problem with nonmatching meshes: undeformed configuration

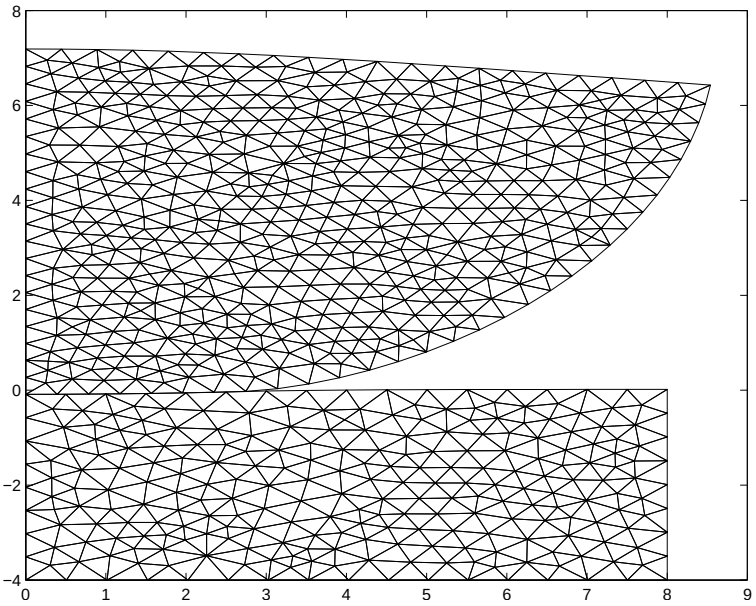

Figure 6: Hertz contact problem with nonmatching meshes: deformed configuration (frictionless case)

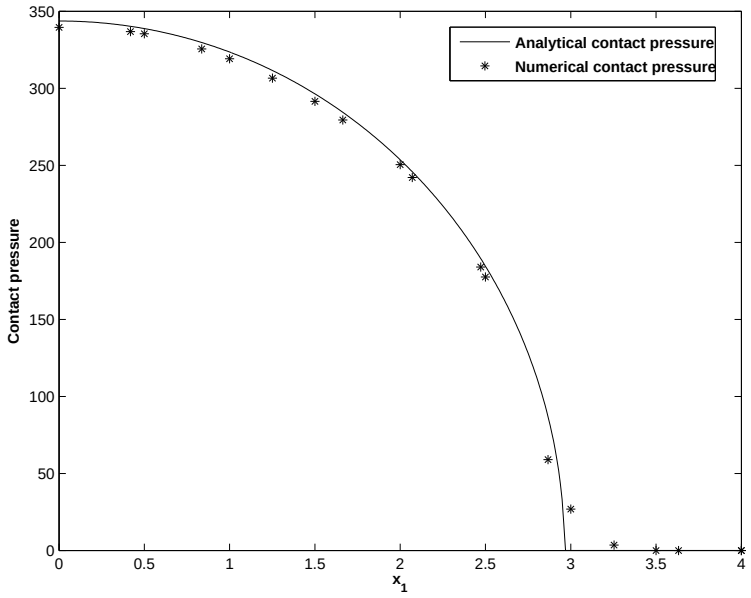

Figure 7: Hertz contact problem with nonmatching meshes: contact pressure (frictionless case)

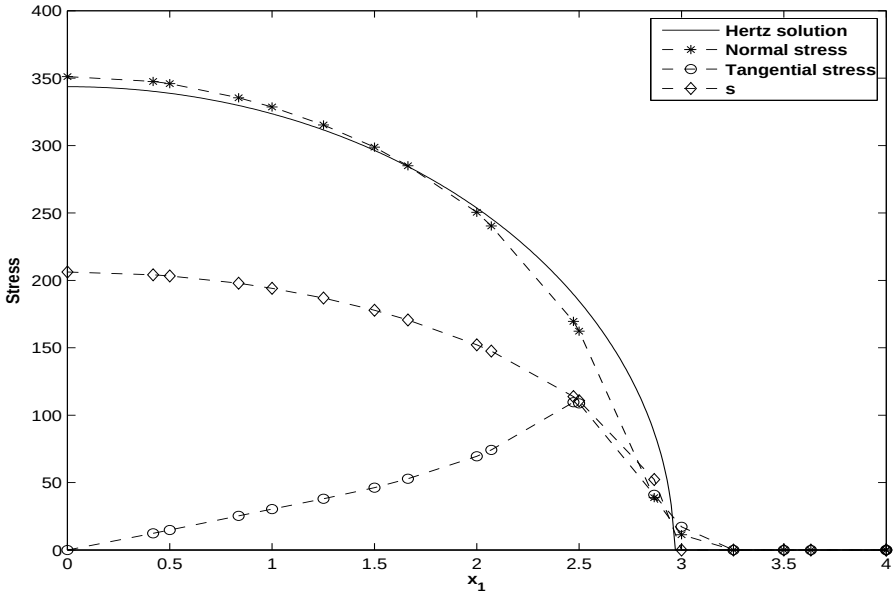

Figure 8: Hertz contact problem with nonmatching meshes: Stress distributions on Γ_c

	Number of iterations	
Interface nodes on $\Gamma_{ch_1}/\Gamma_{ch_1}$	Frictionless case	Friction case
11/9	29	35
21/17	30	39
41/33	31	41
81/65	32	38

Table 2: Performances of Algorithm UBR-DDM on Hertz problem with nonmatching meshes

5.2 Example 2

This example is derived from [16], see Figure 9. We consider the contact problem beetwin two rectangular blocks

$$\Omega^1 = (0,1)^2,\ \Gamma_D^1 = \{1\} \times (0,1),\ \Gamma_N^1 = (0,1) \times \{1\},\ \boldsymbol{g}^1 = \begin{pmatrix} 0 \\ -100 \end{pmatrix}$$

$$\Omega^2 = (0,1) \times (-1,0),\ \Gamma_D^2 = (0,1) \times \{-1\} \cup \{1\} \times (-1,0).$$

The elastic constants are $E^1 = 13000$, $\nu_1 = 0.2$, $E^2 = 30000$ and $\nu_2 = 0.2$. The friction coefficient is $\nu_f = 0.3$. For this problem, we have

$$\Gamma_c^1 = \Gamma_c^2 = \Gamma_c = (0,1) \times \{0\}.$$

The exact solution of this contact problem is a uniform σ_{22} field of value -100 for the frictionless case. For the friction case we set $s = 100\nu_f$.

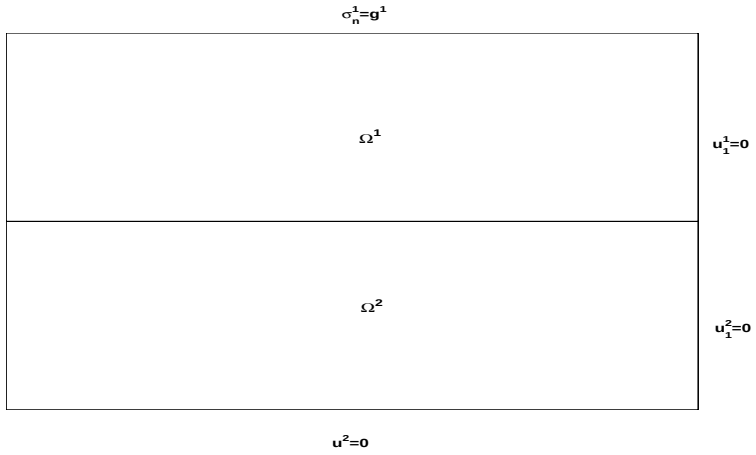

Figure 9: Geometry of the problem

5.2.1 Matching meshes

We first run the Matlab code with a uniform mesh of size 1/8 on the frictionless problem. Figure 10 shows the deformed configuration and the distribution of the vertical component of the stress σ_{22}. The color bar shows that the value of σ_{22} is about -100 within both bodies. Figure 11 depicts the deformed configuration for the case with friction. We notice that the contact beetwin both blocks is in "stick" mode. Figure 12 shows the stress distributions on Γ_c and confirms the "stick" mode since we have $\sigma_t < s = \nu_f|\sigma_n|$ on Γ_c.

For the numerical behavior of the algorithm, the mesh of size 1/8 is successively refined to produce meshes with size 1/16, 1/32, 1/64 and 1/128. The performances of Algorithm UBR-DDM is reported in Table 3. We notice again than the number of iterations is virtually independent of the mesh size.

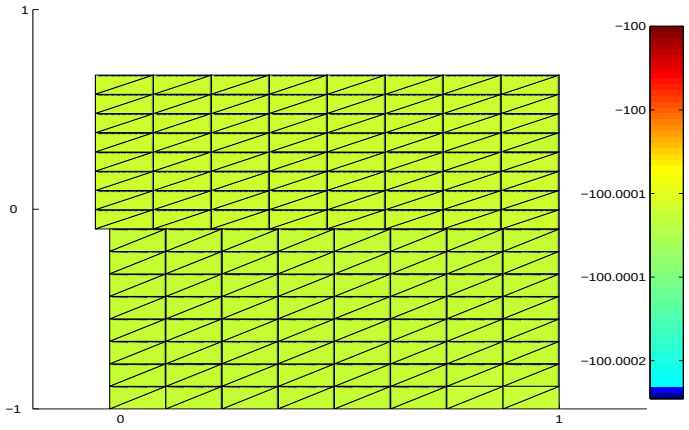

Figure 10: Deformed configuration and σ_{22} distribution for the frictionless case

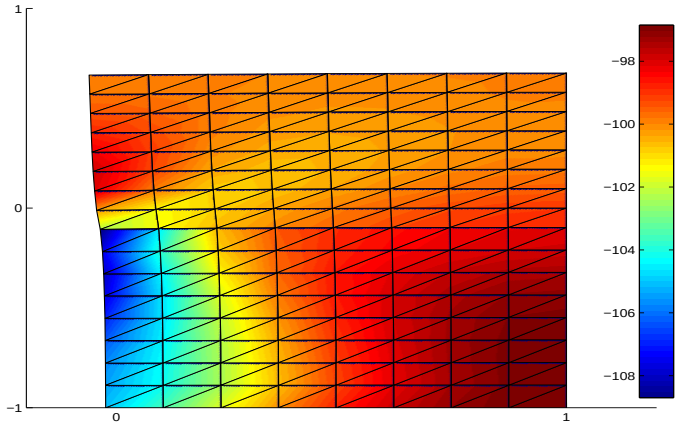

Figure 11: Deformed configuration and σ_{22} distribution for the friction case

	Number of iterations	
Mesh size	Frictionless case	Friction case
1/8	20	42
1/16	20	43
1/32	20	37
1/64	20	34
1/128	20	34

Table 3: Performances of Algorithm UBR-DDM with matching meshes

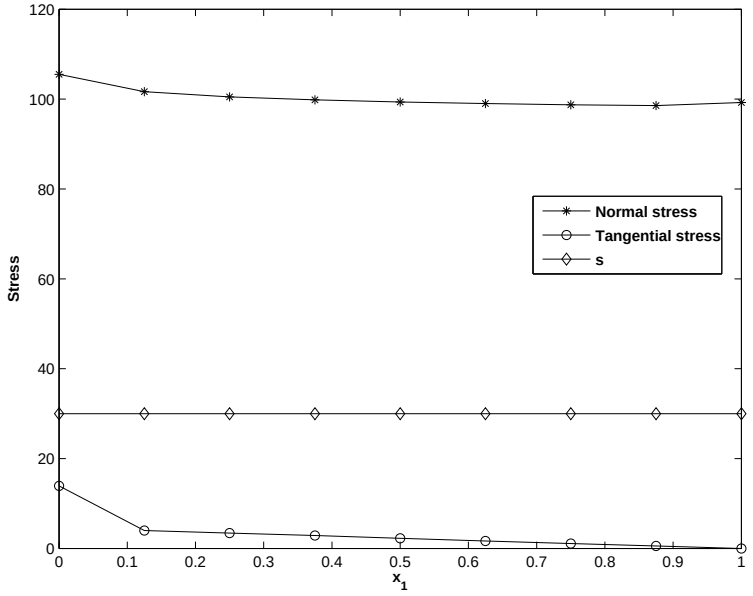

Figure 12: Stress distribution on Γ_c

	Number of iterations	
Interface nodes on $\Gamma_{ch_1}/\Gamma_{ch_1}$	Frictionless case	Friction case
9/5	20	25
17/9	20	30
33/17	20	38
65/33	20	41
129/65	20	40

Table 4: Performances of Algorithm UBR-DDM with nonmatching meshes

5.2.2 Nonmatching meshes

We have also used Algorithm UBR-DDM with a sequence of nonmatching meshes. Figure 13 shows the deformed configuration (friction case), in accordance with Figure 11. We report in Table 4 the performace of Algorithm UBR-DDM. We notice again that the number of iterations is virtually independent of the mesh size.

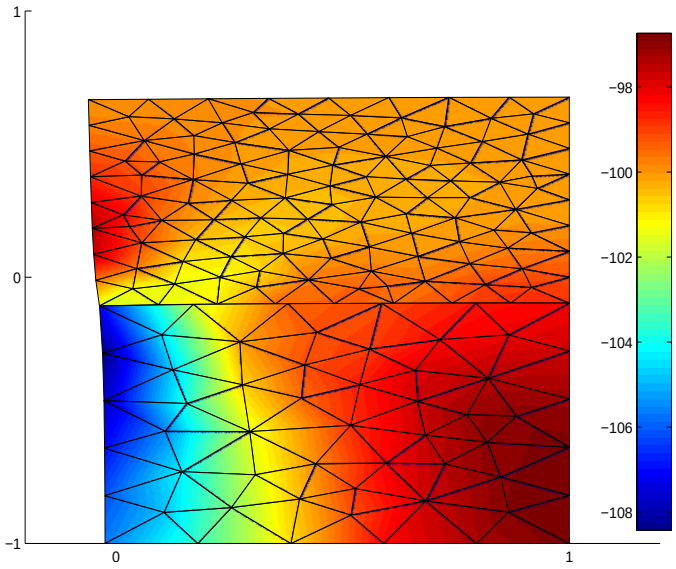

Figure 13: Deformed configuration and σ_{22} distribution for the friction case and nonmatching meshes

5.2.3 Three-dimensional case

We now study the three-dimensional version of the problem. The contact surface becomes

$$\Gamma_c^1 = \Gamma_c^2 = \Gamma_c = (0,1) \times (0,1) \times \{0\}.$$

The exact solution is still a uniform σ_{33} field of value -100 for the frictionless case. For the friction case we set $s(x) = 100\nu_f$ on Γ_c.

Figure 14 shows a uniform mesh sample of size 1/4 while Figure 15 shows the deformed configuration in accordance with the two-dimensional results. We report in Table 5 the performances of the algorithm showing its scalability.

6 Conclusion

We have studied a new domain decomposition method for the two-body contact problem with Tresca friction. Numerical experiments have shown that the algorithm is scalable

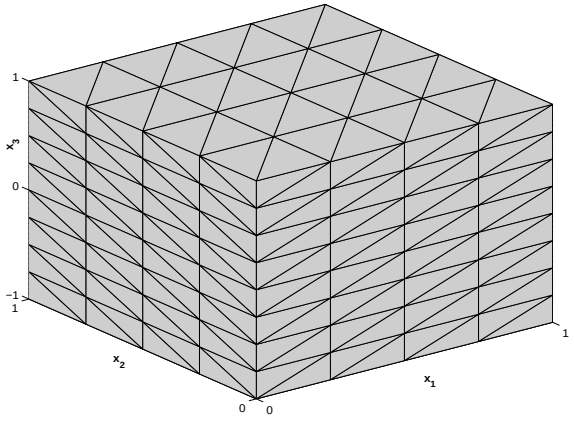

Figure 14: Mesh sample of size 1/4 for the three dimensional contact problem

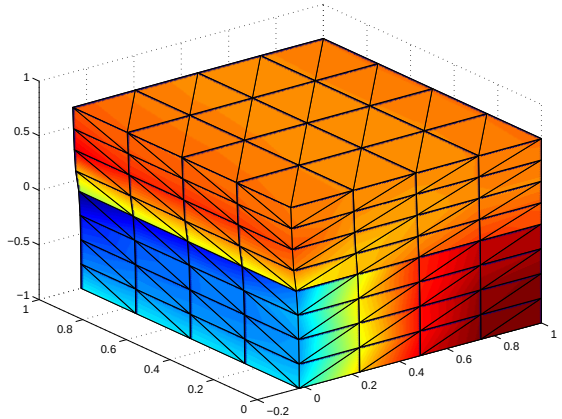

Figure 15: Deformed configuration and σ_{33} distribution for the problem with friction

	Number of iterations	
Mesh size	Frictionless case	Friction case
1/4	20	34
1/8	20	42
1/16	20	43
1/32	20	43

Table 5: Performances of Algorithm UBR-DDM on a three-dimensional problem

with matching or nonmatching meshes.

To reduce the size of the linear elasticity subproblems, the standard domain decomposition constraints can be added to the constrained optimization problem (3.1)-(3.3) for each subdomain. Using a three-field formulation, see e.g. [26, 27], we can derive a Uzawa block relaxation domain decomposition method with "small" subdomain problems.

References

[1] Bayada G., Sabil J. and Sassi T. Algorithme de Neumann-Dirichlet pour des problèmes de contact unilateral: Résultat de convergence. *C. R. Acad. Sci. Paris, Ser. I*, 335:381–386, 2002.

[2] Bayada G., Sabil J. and Sassi T. A Neumann-Neumann domain decomposition algorithm for the Signorini problem. *Appl. Math. Lett.*, 17:1153–1159, 2004.

[3] Bertsekas D. *Constrained Optimization and Lagrange Multipliers Methods*. Academic Press, New York, 1982.

[4] Bertsekas D. *Nonlinear Programming*. Athena Scientific, Nashua, NH, 1999.

[5] Cea J. and Glowinski R. Sur des méthodes d'optimisation par relaxation. *R.A.I.R.O.*, R-3:5–32, 1973.

[6] Dostál Z. and Horák D. Scalable FETI with optimal dual penalty for variational inequalities. *Numer. Linear Algebra Appl.*, 11:455–472, 2004.

[7] Dostál Z., Gomes Neto F. A. M. and Santos S. A. Solution of contact problems by FETI domain decomposition with natural coarse space projection. *Comput. Methods. Appl. Mech. Engrg.*, 190:1611–1627, 2000.

[8] Dostál Z., Haslinger J. and Kučera R. Implementation of the fixed point method in contact problems with Coulomb friction based on a dual splitting type technique. *J. Comput. Appl. Math.*, 140:245–256, 2002.

[9] Dureisseix D. and Farhat C. A numerically scalable domain decomposition method for solution of frictionless contact problems. *Internat. J. Numer. Methods Engrg*, 50:2643–2666, 2001).

[10] Ekland I. and Temam R. *Convex Analysis and Variational Problems*. Classics in Applied Mathematics. SIAM, Philadelphia, 1999.

[11] Farhat C. and Roux F. X. A method of finite element reearing and interconnecting and its parallel solution algorithm. *Internat. J. Numer. Methods Engrg*, 32:1205–1227, 1991.

[12] Fortin M. and Glowinski R. *Augmented Lagrangian Methods: Application to the Numerical Solution of Boundary-Value Problems*. North-Holland, Amsterdam, 1983.

[13] Glowinski R. and Le Tallec P. *Augmented Lagrangian and Operator-splitting Methods in Nonlinear Mechanics*. Studies in Applied Mathematics. SIAM, Philadelphia, 1989.

[14] Goldsmith W. *Impact*. Edward Arnold, London, 1960.

[15] Haslinger J., Dostál Z. and Kučera R. On the splitting type algorithm for the numerical realization of the contact problems with Coulomb friction. *Comput. Methods. Appl. Mech. Engrg.*, 191:2261–2281, 2002.

[16] Hild P. Numerical implementation of two noncoforming finite element methods for unilateral contact. *Comput. Methods. Appl. Mech. Engrg.*, 184:99–123, 2000.

[17] Ito K. and Kunisch K. The augmented lagrangian method for equality and inequality constraints in Hilbert scpaces. *Math. Program.*, 46:341–360, 1990.

[18] Johnson K.L. *Contact Mechanics*. Cambridge University Press, Cambridge, 1987.

[19] Kikuchi N. and Oden J.T. *Contact problems in Elasticity: A Study of Variational Inequalities and Finite Element Methods*. Studies in Applied Mathematics. SIAM, Philadelphia, 1988.

[20] Koko J. An optimization based domain decomposition method for a two-body contact problem. *Numer. Funct. Anal. Optim.*, 24(5-6):587–605, 2003.

[21] Koko J. Lagrange multiplier based domain decomposition methods for a nonlinear sedimentary basin problem. *Comput. Geosci.*, 2007. To appear.

[22] Koko J. Vectorized Matlab codes for two-dimensional linear elasticity. *Scientific Programming*, 2007. To appear.

[23] Kosior F., Guyot N. and Maurice G. Analysis of frictional contact problem using boundary element method and domain decomposition method. *Internat. J. Numer. Methods Engrg.*, 46:65–82, 1999.

[24] Licht C., Pratt E. and Raous M. Remarks on a numerical method for unilateral contact including friction. In *Unilateral problems in structural analysis*, volume 101 of *Internat. Ser. Numer. Math.*, pages 129–144. Birkh$'$auser, Nasel, 1991.

[25] Luenberger D. *Linear and Nonlinear Programming*. Addison Wesley, Reading, MA, 1989.

[26] Magoulès F. and Roux F.-X. Lagrangian formulation of domain decomposition methods: A unified theory. *Appl. Math. Modelling*, 30:593–615, 2006.

[27] Quarteroni A. and Valli A. *Domain Decomposition Methods for Partial Differential Equations*. Oxford University Press, 1999.

[28] Schöberl J. Solving the Signorini problem on the basis of domain decomposition techniques. *Computing*, 60:323–244, 1998.

[29] Wriggers P. and Simo J.C. A note on tangent stiffness for fully nonlinear contact problems. *Comm. in Appl. Num. Methods*, 1:199–203, 1985.

[30] Zavarise G. and Wriggers P. A segment-to-segment contact strategy. *Mathl. Comput. Modelling*, 28:497–515, 1998.

[31] Zavarise G., Wriggers P., Stein E. and Schrefler B.A. Real contact mechanisms and finite element formulation–A coupled thermomechanical approach. *Internat. J. Numer. Methods Engrg*, 35:767–785, 1992.